JOURNAL OF MATERIALS SCIENCE 14 (1979) 1707–1716

Reinforcement of mortar with Metglas* fibres

A. S. ARGON, G. W. HAWKINS, H. Y. KUO
Massachusetts Institute of Technology, Cambridge, Mass. 02139 USA

An alkali resistant Metglas fibre of composition $Fe_{29}Ni_{49}P_{14}B_6Si_2$ was used in 2.5 cm lengths as discontinuous reinforcement for mortar. The force–displacement curves for pull-out of roughened individual fibres embedded into mortar were measured. Composite experiments with fibres in planar random orientations have demonstrated that the first crack strength rises weakly with increasing fibre volume fraction according to the principle of non-propagating cracks. The maximum post cracking strength rises linearly with increasing volume fraction up to $V_f = 0.012$ where it levels off due to secondary fragmentation in the matrix. The monotonic fracture behaviour of the material in nearly all respects is in accord with theoretical expectations. Under cyclic conditions, the composite undergoes progressive damage only when the maximum tensile stress per cycle penetrates beyond a critical amount into the range between the first crack strength and the maximum post-cracking strength.

1. Introduction

Cement, mortar and concrete by themselves have low tensile strength and low fracture toughness. In large scale construction, they are always reinforced and often pre-stressed by large diameter steel bars. In many other applications involving panels, thin sections and durable surface coatings, and for protection against small scale fragmentation, the reinforcement of cementitious materials with a variety of strong and stiff elastic fibres, such as asbestos, glass, and steel, has been widespread. As has been discussed by Krenchel [1], of these fibres, asbestos have been preferred for many years. Due to the depletion of high grade, long asbestos fibres, and due to health hazards they create, alternatives such as fibres of alkali-resistant glass, steel, carbon, and even some polymers have been considered. Details of such uses can be found in the proceedings of recent international conferences [2–5]. Here we will present a study of the use of corrosion resistant metallic glass fibres for reinforcement of cement.

2. Recapitulation of the theory of fibre reinforcement

The fundamental issues of reinforcement of brittle and fragile cementitious materials by both continuous and discontinuous strong and stiff fibres have recently been critically reviewed by Argon and Shack [6]. From both the point of view of economics and the difficulty of mixing long fibres into concrete, usually only relatively small volume fractions of fibre ($\sim$ 2 to 5%) are considered. Under these circumstances it has been established that the beneficial effects of increased fracture work result primarily from the frictional work of fibre pull-out when the cementitious matrix cracks. The fibres bridging the crack delaminate from the matrix, and are subsequently pulled out from the crack flanks under continued straining. This necessitates that the fibres have Young's moduli higher than that of the cement, and do not yield or fracture before the delamination zone between fibre and cement travels up along the fibre to initiate pull-out.

The usually small volume fractions of fibres and their relatively modest excess of Young's modulus over that of the cement, means that the change in overall stiffness of the composite is usually not noteworthy. The fibres, however, can provide an increase in the first crack strength, below which cracks of any length cannot propagate in the matrix for energetic reasons. In a cementitious composite, this stress σ_c, below which cracks

* Registered trademark of Allied Chemical Corporation.

0022–2461/79/071707–10 $3.00/0

in the matrix cannot propagate, is given by [6],

$$\sigma_c = \left[\eta V_f\left(\frac{E_f}{E_m}\eta V_f + 1\right)\right]^{2/3}\left[\frac{12\alpha\tau_b E_f}{r(1-\eta V_f)}\right]^{1/3}, \quad (1)$$

where V_f, E_f and r are the volume fraction, Young's modulus and thickness of the fibres or ribbon-shaped reinforcement; E_m and α, the Young's modulus and fracture surface energy of the cementitious matrix; and finally τ_b, the frictional shear traction between fibre and matrix during fibre pull-out. In Equation 1, η is the fibre efficiency factor which is unity for continuous fibres aligned parallel to the tension axis and 0.41 for discontinuous straight fibres with a random orientation in space in a composite with an average Poisson's ratio of 0.3, as was demonstrated by Romualdi and Mandel [7]. In a composite with fibres arranged to be isotropic in a plane, and loaded in tension in that plane, this efficiency becomes 0.58, as can be readily demonstrated by an extension of the analysis of Romualdi and Mandel. When the volume fraction V_f is too small to result in σ_c values smaller than the inherent strength f_m of the unreinforced matrix, the latter will supercede, and the larger of the two will always govern the first crack strength f_{fc}, i.e.

$$f_{fc} = f_m \quad (\text{for } f_m > \sigma_c), \quad (2a)$$

$$f_{fc} = \sigma_c \quad (\text{for } \sigma_c > f_m). \quad (2b)$$

For the composite to remain intact after formation of the first matrix cracks, the fibres must bear the entire load without entirely delaminating from the matrix. This requires a minimum combination of volume fraction V_f, fibre length l, fibre periphery s, and fibre cross-sectional area A_f, given by

$$sl\eta' V_f\tau_b/4A_f \geqslant f_{fc}, \quad (3)$$

and a fibre strength in excess of

$$f_f > f_{fc}/V_f\eta' \quad (4)$$

where η', the efficiency of discontinuous fibres after first cracking will be very nearly unity regardless of orientation. This is because once pull-out begins, fibres must bend and bridge across the crack parallel to the tension axis, resulting in nearly equal frictional pull-out work for fibres of all orientations except those nearly parallel to the crack faces, which are likely to fracture away from the matrix. If these two conditions can be met, the stress must be raised further to separate the cracked part, giving an apparent hardening behaviour for the composite. In Equation 3, the term on the left hand side is the maximum post-cracking strength of the composite

$$f_{cu} = sl\eta' V_f\tau_b/4A_f. \quad (3a)$$

When the inequality in Equation 3 is reversed, the maximum post-cracking strength will be less than the first crack strength and the composite will begin to fracture under decreasing traction immediately upon the first cracking event.

In a properly designed composite with discontinuous fibres, the fibres are chosen to have an optimum length l_0 for which the entire pull-out traction over the most probable pull-out length of $l/4$ is just short of the fibre strength, f_f, i.e.

$$l_0 \leqslant \frac{4A_f f_f}{s\tau_b}. \quad (5)$$

Ideally, when the maximum post-cracking strength is reached and the cracked composite is separated by pulling out fibres from the flanks of the crack, the overall traction should linearly decrease to zero over the most probable pull-out distance of $l/4$. Thus, the effective specific fracture work α' per unit projected surface area created will be

$$\alpha' = f_{cu}l/16 = \frac{sl^2\eta' V_f\tau_b}{64A_f}. \quad (6)$$

In reality, fibre pull-out distances will vary from nearly zero to $l/2$. This and a likely degradation of the frictional traction along the fibre with increasing pull-out will make the actual specific fracture work less than that given in Equation 6.

The fracture toughness K_{Ic} is normally very difficult to measure for a composite with long fibres. This manifests itself by an absence of notch sensitivity in laboratory samples, which has been a source of confusion to some investigators. The problem is well known in fracture mechanics, and, as was clarified by Argon and Shack [6], is a direct result of the fibre pull-out mode of fracture that makes the critical crack opening displacement (CCOD) fully $l/4$. Thus a properly designed "linear–elastic–fracture-mechanics" experiment requires that CCOD $\ll R \ll c \ll w$, where R, c, and w are the fracture process zone (apparent "plastic" zone), the crack length and specimen

width respectively. Since CCOD = $l/4$ is commonly in the range of 0.5 cm, a properly designed fracture toughness experiment would require a specimen of about 5 m width containing a crack of 0.5 m – hardly an easy configuration for common laboratory experiments. Therefore, no attempt was made in this investigation to measure the fracture toughness K_{Ic} of composite samples.

3. Experimental procedure

3.1. Mortar

The mortar used in this investigation was prepared according to ASTM C-190 standards. It consisted by weight of: 65% graded sand that was made up mostly of quartz grains of 0.035 cm diameter; 24% high early strength Type III Portland cement, made by the Martin Marietta Co., and 11% water. Fibres were added after the dry ingredients were mixed but before the water was added. After mixing was complete, the mortar was poured into moulds which were usually of a shape to make flat rectangular plates. When the moulds were filled, they were vibrated on a shaker table to eliminate major air bubbles. The moulds were then covered with wet paper towels and a plastic sheet to retain the moisture, and were cured for 24 h. This cure was followed for 6 days or more by a cure in tanks filled with lime-water. All tests of the specimens were performed in a wet condition, usually immediately after the customary 7 day cure. The tensile strength of the unreinforced mortar was measured by means of standard dog-bone shaped specimens, tested at different stress rates ranging from 0.2 MPa min^{-1} to 20 MPa min^{-1}. This showed an increasing strength that was logarithmic in stress rate, ranging from 2.36 to 4.0 MPa. A tensile strength value of 3.2 MPa obtained for a stress rate of 2 MPa min^{-1} will be considered here as the average base strength of the unreinforced mortar. The compressive strength of the mortar measured on cubical specimens of 5 cm edge length was found to be 39.4 MPa.

3.2. Metglas fibre

The reinforcing material used was Metglas fibre, made by the Allied Chemical Corporation, with a designation of 2826B and a composition of $Fe_{29}Ni_{49}P_{14}B_6Si_2$. This is resistant to corrosion – particularly by the constituents of the mortar. As with most melt spun filaments, the fibre had a thin air-foil shaped cross-section with a width of 0.053 cm, a thickness of 7.8×10^{-3} cm (area of 3.18×10^{-4} cm^2), and a periphery of 0.117 cm. This gave the fibres a periphery to square root area ratio of 6.583: that is 1.86 times that of a fibre of circular cross-section. The as-received fibre had one smooth and slightly crowned side, shown

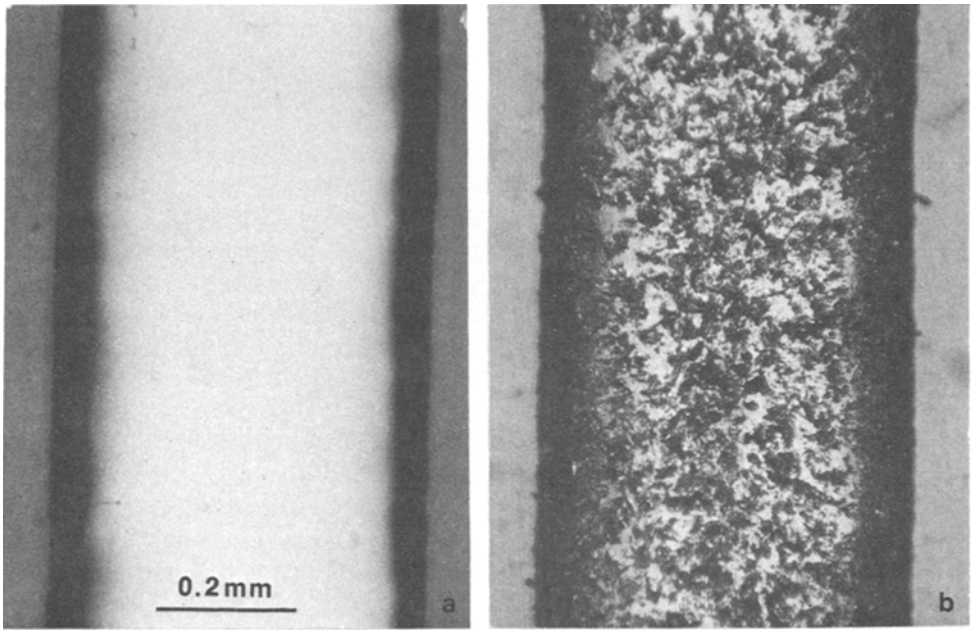

Figure 1(a) Appearance of crowned side of Metglas fibre produced by melt spinning; (b) appearance of same side of fibre after sand blasting.

in Fig. 1a, while the other side was flat but showing the longitudinal machining marks of the cold drum on which it was cast.

Tests on individual fibre segments showed that they had a Young's modulus of 127 GPa and a tensile strength of 2.3 GPa. The fibres were sand blasted to roughen them to increase their effective pull-out traction. This produced a deeply pitted surface as shown in Fig. 1b. Tension tests carried out with such sand blasted fibres showed no measurable decrease in tensile strength.

Tests with individual fibres required special considerations to avoid stress concentrations in gripping. In such instances, fibres were loaded by wrapping their ends on two separate large mandrels which were part of a special grip arrangement. The gradual build-up of frictional tractions along the periphery of the mandrels prevented stress concentrations there and assured fracture away from the grip sections – even in fibres with no special narrow gauge sections. In individual fibre pull-out tests, good results were obtained by gripping the fibre close to its site of emergence from the mortar by means of a specially constructed grip incorporating a modified parallel sided, flat faced "Vice-grip" plier.

3.3. Mortar–Metglas composite tension specimens

Based on the results of fibre pull-out tests to be discussed in the next section, the optimum fibre length l_0, computed from Equation 5 by using the given fibre geometry, was found to be nearly 2.5 cm for the sand blasted fibres. In all composite tension and cyclic loading tests this was the length of fibre used.

The mixed mortar containing the desired volume fraction of fibres was poured into flat moulds to a thickness of 1 cm to produce large plate-like slabs of a desired nominal fibre volume fraction. The poured mixture in such flat moulds was first packed down with vertical strokes of a horizontal metal bar to obtain a uniform thickness with a high quality surface closing over all fibres, and was subsequently vibrated on a shaker table to release any remaining large bubbles. This was followed by another round of packing down. This procedure tended to disperse fibres randomly in the plane with no preferred orientation except in a boundary zone of about 1 cm thickness at the edges of the large plate mould. This thin layer was removed after the customary 7 day cure and did not become a part of the specimens. After the 7 day cure, twelve tension specimens with dimensions of 3.75 cm width and 8.75 cm length with 1 cm thickness could be cut out of a given plate by a diamond cut-off wheel of 1.5 mm thickness. Specimens were notched at their centre from both sides to a depth of 5 mm with the same cut-off wheel to localize the fracture at the centre of the specimen and to make specimen separation displacements readily measureable. As discussed in Section 2, such notches on specimens of the given dimensions merely serve to reduce the net section without introducing any significant notch weakening. Although the large slabs were prepared in order to have a discrete set of volume fractions of fibres, the actual volume fraction in the waists of the individual specimens over a cross-sectional area of only 2.75 cm^2 differed significantly from the overall average. Hence in each case, the actual volume fraction of fibre crossing the waist in each specimen was determined by direct fibre counts on the fracture surface after the experiment was over.

Wedge shaped end blocks of plaster of Paris were glued at both sides of all specimens, to permit trouble free loading of specimens in grips with tapered openings. The grips used for testing the specimens in tension and in repeated tension cycling were constructed according to the ASTM C–190 standards with only minor modification. No difficulty due to either eccentric loading or breakage away from the narrowed mid-section was encountered.

4. Experimental results

4.1. Fibre pull-out tests

As mentioned in Section 2, the main source of toughness in fibre-reinforced mortar and concrete is the energy dissipated in the process of pulling out fibres from the flanks of cracks that form in the matrix at the first crack strength. Hence, the fundamental information for such materials is the force–displacement curve resulting from pulling out individual fibres embedded into a semi-infinite mortar or concrete medium.

When the lengths of individual fibres embedded into a large block of mortar, are pulled out by grips which grasp the fibres as near as possible to the surface of the mortar, the force–displacement curves that result are found to have two stages. This is shown in Fig. 2 for a typical sand blasted fibre. In the first stage, the force builds

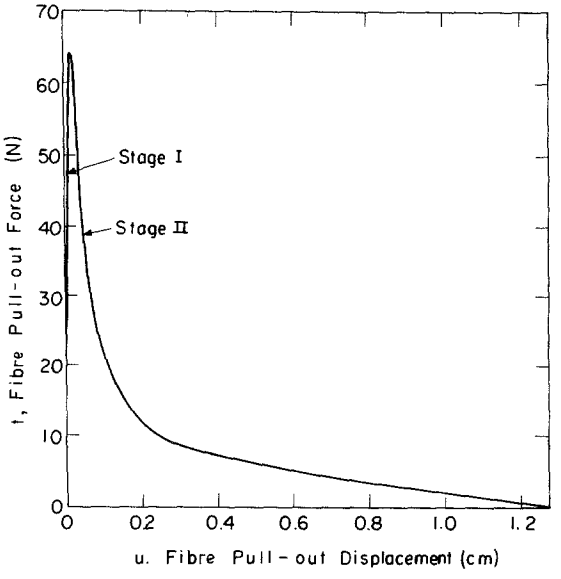

Figure 2 Force–displacement curve of roughened fibre being pulled out of mortar, showing two stages of pull-out resistance. The peak occurs when delamination along fibre reaches fibre end.

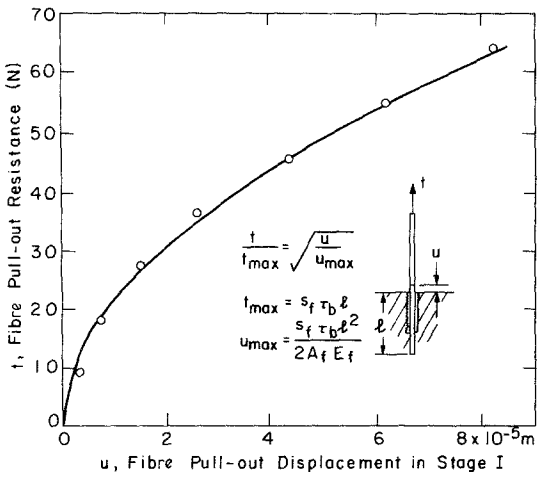

Figure 3 Stage I of fibre pull-out, showing a parabolic dependence of pull-out resistance on fibre end displacement.

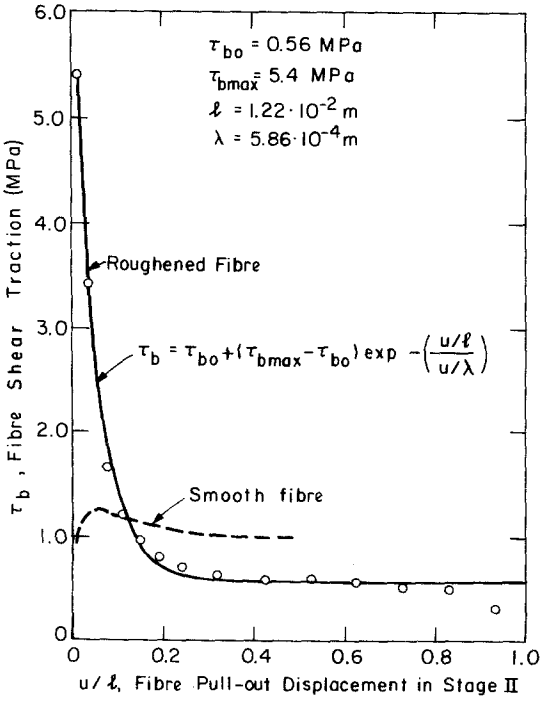

Figure 4 Degradation of interface shear traction with relative displacement of a roughened fibre drawn out of a mortar matrix.

up rapidly with small amounts of fibre end displacement. During this stage, a delamination front is initiated from the free surface and propagates gradually toward the extreme end of the fibre embedded in the matrix. If, in the delaminated portion of the interface, a constant shear traction τ_b is maintained along the fibre surface, the resulting force–displacement curve, $t(u)$, will be in the form of a parabola as shown in Fig. 3 for a roughened fibre, given by

$$t = \sqrt{(2s\tau_b A_f E_f u)}. \quad (7)$$

In Equation 7, s, A_f, and E_f are the periphery, cross-sectional area and Young's modulus of the fibre, while t and u are the tensile pull-out force and end displacement, respectively. The force reaches a maximum t_{max} at a displacement u_{max} given by

$$t_{max} = s\tau_b l \quad (8a)$$

$$u_{max} = s\tau_b l^2/2A_f E_f \quad (8b)$$

when the delamination front arrives at the end of the fibre at a depth l. Fig. 3 shows a parabolic equation fitted to the data points of a Stage I pull-out process of a roughened fibre of 1.22 cm embedded length, at a pull-out velocity of 0.05 cm min^{-1}. The data and the fitted curve according to Equations 7 and 8 indicate that the maximum shear traction along the fibre–mortar interface $\tau_b = 5.4$ MPa. This is very closely similar to the shear tractions reported by Majumdar [8] for both clean and rusty mild steel in concrete.

When the delamination is complete, Stage II begins and the fibre starts to be pulled out. If the shear traction along the fibre–mortar interface were to remain constant, the force–displacement curve in Stage II pull-out would show a linear drop

to zero. The curve in Fig. 2, however, shows a much more rapid drop upon initial pull-out which indicates that the shear traction degrades with relative displacement between fibre and matrix. The actual magnitude of the average shear traction τ_b was determined from the magnitude of the measured force and known length of fibre engagement, and is plotted in Fig. 4 as a function of relative fibre displacement. The decay is nearly exponential with a characteristic decay distance of λ, that is, of the order of the sand grain size in the mortar or of the wave length of roughness of the sand blasted fibre surface. This suggests that a fragmented layer with roller-like particles forms upon displacement of the fibre by one sand grain diameter. The details of a very similar fibre interface degradation process have been observed and documented metallographically by Pinchin and Tabor [9]. In Fig. 4, the smooth fibre shows a very much lower maximum shear traction which, however, does not degrade with relative fibre displacement. The two stage pull-out behaviour shown in Fig. 2 was found to be quite reproducible in a large number of individual fibre pull-out experiments.

The effect of speed on pull-out was negligible during Stage I. During Stage II, increased pull-out speed produced some reduction in pull-out traction. This effect too, however, was minor and was not investigated further.

4.2. Monotonic tension experiments

Notched rectangular samples with tapered ends containing nominal volume fractions of fibre ranging from 0 to 0.03 were tested in tension at a nominal grip displacement rate of 0.05 cm min^{-1}. As already described above, such specimens were provided with a pair of opposing shallow notches to localize the fracture event in the centre of the specimen. The opening displacements of specimens were measured with a conventional clip-on gauge used in measurement of crack opening displacements.

When specimens of the type described with fibre volume fractions $V_f \leqslant 0.03$, are loaded, the "first cracking" event occurs only at the narrowed waists and the specimens are eventually torn apart at this plane without the appearance of other cracks elsewhere. This measures the actual behaviour of separation and establishes unambiguously the specific fracture work. Thus, these experiments differ fundamentally from those of

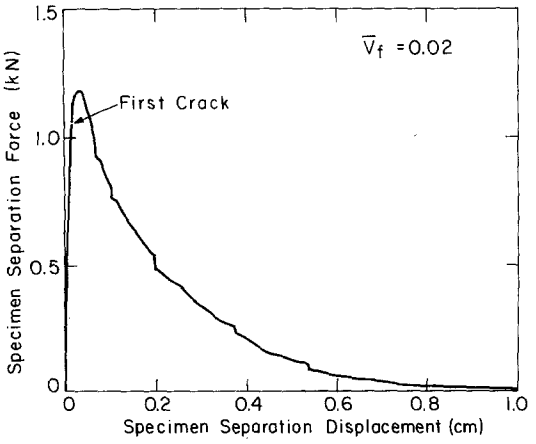

Figure 5 Specimen separation force versus separation displacement for a composite specimen with a volume fraction of 0.02 of fibres.

Cooper and Sillwood [10] where long slabs having continuous fibre reinforcement become multiply cracked in the matrix before finally tearing apart by a series of fractures in reinforcing elements in and around one of the many parallel cracks in the matrix. This last experiment gives a better measure of the overall "elastic–plastic" slab performance prior to the final tearing apart event, while our experiment was particularly designed to determine the specific fracture or tearing work in a composite with discontinuous fibres.

A typical curve of specimen separation force versus separation displacement is shown in Fig. 5 for a sample with a nominal fibre volume fraction of 0.02. The curve shows that for this volume fraction, the maximum post-cracking strength of the composite f_{cu} is larger than the first crack strength f_{fc}, requiring additional stress on the specimen to complete the spread of the fibre delamination process along the fibre interfaces away from the surfaces of the matrix crack. When such delamination is complete, the tearing begins by pulling out the tufts of fibres from both sides of the crack under decreasing overall traction. As mentioned in Section 3.3. above, the actual fibre volume fraction in the waists of individual specimens was determined from the fracture surfaces after the experiments were over.

Fig. 6 shows the measured first crack strengths of all specimens plotted against $F(V_f)$, the volume fraction function of reinforcements appearing in Equation 1, which was evaluated for a fibre efficiency factor $\eta = 0.58$ on the basis of the planar random nature of the fibres. As can be seen, the

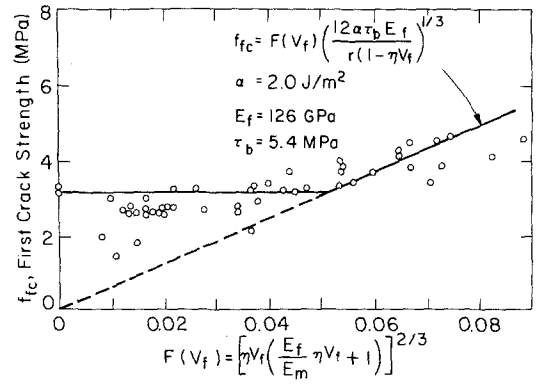

Figure 6 Dependence of first crack strength on volume fraction of fibres, relative stiffness of fibre and matrix and interfacial shear tractions.

measured values follow roughly along the discontinuous behaviour given by Equations 2a and b but are subject to considerable scatter over the entire range. Some of this, no doubt, is a result of the relatively small waist section of the specimen on the scale of the average inter-fibre spacing. The theoretical behaviour shown by the kinked solid line was evaluated using the measured fibre modulus, E_f, maximum pull-out shear traction, τ_b, the average fibre-ribbon thickness, r, and a value α, of matrix surface energy, considered appropriate for a hard but porous inorganic solid held together with primary covalent bonds, and a E_f/E_m ratio of 6.

The measured maximum post cracking strengths f_{cu} are plotted against the fibre volume fraction in Fig. 7. It is seen that f_{cu} does initially increase linearly with increasing V_f as required by Equation

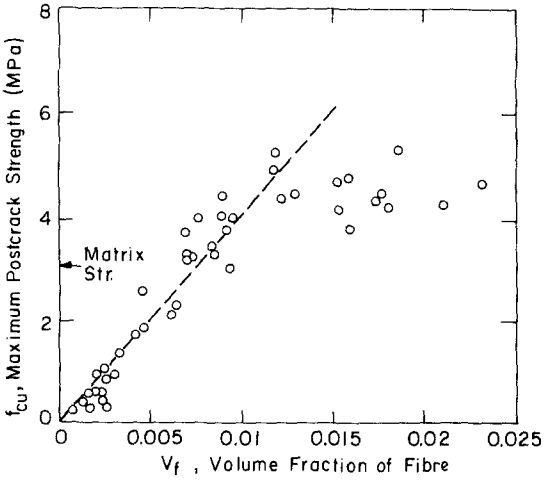

Figure 7 Dependence of maximum post-cracking strength on volume fraction of fibres.

3a. The slope of the dotted line in Fig. 7 is 400 MPa, while the slope predicted by Equation 3a is $df_{cu}/dV_f = 1242$ MPa based on the given fibre dimensions, the measured maximum pull-out shear traction of τ_b and a post cracking fibre efficiency $\eta' \simeq 1.0$, as discussed in Section 2 above. The actual slope is thus only 32% of the expected slope. The reason for this is directly due to the degradation of the shear traction τ_b on fibre pull-out. As is shown in Fig. 4, upon pull-out of only 10% of the engaged length of the fibre, the shear traction drops to about 11% of its peak value. Since all fibres do not begin to pull out simultaneously at the maximum post cracking strength, but instead over a range of displacements governed by the compliance of their engaged lengths, it is quite likely that an average of the effective shear traction over all fibres at the force maximum will be about 1/3. Another estimate based on overall averaged behaviour of fibres during pull-out can be obtained by computing the ratio of the area under the solid curve for the roughened fibre in Fig. 2 to that of the triangle obtained by connecting the peak value of the curve to the value $u/l = 1.0$, i.e. the reference pull-out work of a fibre with truly constant shear traction. This ratio is 0.35.

Examination of Fig. 7 shows more importantly that above a volume fraction of about 0.012, the maximum post cracking strength levels off and only increases very slightly. The reason for this limitation in performance becomes clear upon examination of the region around the fracture. When the volume fraction of fibres increases and the mean distance between the fibres decreases, more and more points exist where combined fibre shear tractions produce stresses in the narrow matrix regions between fibres that exceed the tensile strength of the mortar, resulting in the premature removal of chunks of mortar stuck between these fibres. This is observable as an increase in the tortuosity of the fracture path and as an increase of fragmentation near the fracture surface. It indicates that, for the given fibre dimensions and interface traction, no further improvement in performance is obtained for fibre volume fractions in excess of about 0.015.

The specific work for fracture α' for tearing the specimen apart can be obtained by computing the area under the overall traction–displacement curve for a specimen such as that given in Fig. 5. For a volume fraction of 0.01, this is found to

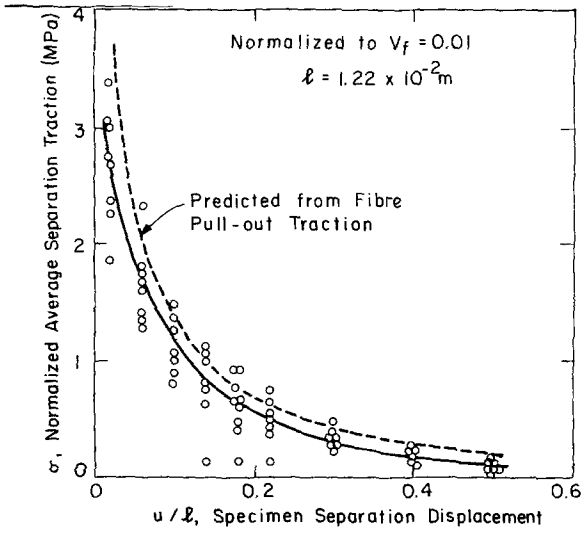

Figure 8 Measured specimen separation traction and computed separation traction based on individual force–displacement curves for fibre pull-out.

be $\alpha' = 4660\,\mathrm{J\,m^{-2}}$. When the expression in Equation 6 is evaluated with due consideration for degradation of the interface shear traction which was discussed above, a value of $5821\,\mathrm{J\,m^{-2}}$ is obtained which is considered to be in good agreement with the experimental figure. Considering that the specific fracture work for the unreinforced mortar may be only of the order of $2\,\mathrm{J\,m^{-2}}$, the introduction of 0.01 volume fraction of reinforcement by Metglas fibres gives a 2300 fold increase in the specific fracture work.

Finally, it is possible to demonstrate that the fundamental force–displacement relation such as that shown in Fig. 2, measured in individual fibre pull-out experiments, accounts very well for the form of the specimen separation force with increasing separation displacement. The latter curve can be readily computed from the known individual fibre curves if it is assumed that a randomly placed crack will touch a definite number of fibres and will divide them randomly into two parts of unequal length engaged into opposite faces of the crack. Of these, the short one will have equal probability of being between zero length and $l/2$. Thus the overall specimen separation traction will be made up of a superposition of the force–displacement curves of such fibres with a continuous and constant distribution of engaged lengths between zero and $l/2$. When this is done and the results are compared with actual experimental curves of a variety of specimens, all normalized to a constant fibre volume fraction of $V_f = 0.01$, Fig. 8 is obtained. It is seen that the overall average of the experimental specimen traction–displacement curve lies a little below the theoretical curve obtained by the superposition of the individual fibre pull-out curves described above. This indicates that the fibre efficiency η' is indeed very nearly unity.

4.3. Cyclic tension experiments

Based on the findings of the monotonic tension experiments, a limited number of cyclic tension experiments were also performed to explore the fatigue behaviour of fibre-reinforced mortar. These experiments were all performed on specimens with a nominal volume fraction of reinforcement of 0.015, which were shaped identically to the monotonic tension specimens using the same ASTM C–190 gripping procedure. The experiments were performed on an Instron machine in a tension–tension mode, with a saw tooth waveform at a frequency of about 3 cycles $\mathrm{min^{-1}}$. The minimum stress in every cycle was 0.48 MPa. These specimens were also equipped with a clip-on gauge across the narrowed waist section to monitor any degradation of behaviour.

Cycling to just below the first crack strength in uncracked specimens did not produce any detectable change over 1000 cycles. As a result it was decided that all specimens would first be monotonically taken to their first crack strength and subsequently cycled at various stress levels. In such pre-cracked samples, cycling below the first crack strength again produced no detectable change over 1000 cycles. Hence it was decided to cycle the pre-cracked specimens to maximum stresses above the first crack strength.

In total, 16 specimens were cycled to maximum stresses between 1.0 to 1.5 times the first crack strength. These specimens lasted anywhere between 1 cycle to above 1000 cycles and exhibited at first

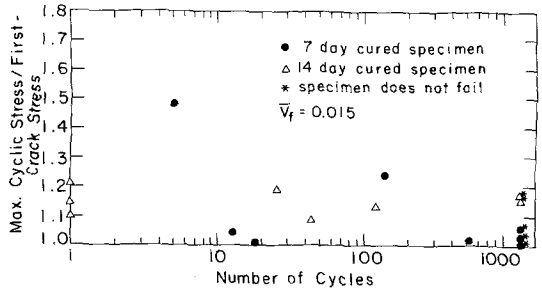

Figure 9 Dependence of specimen life on the magnitude of maximum cyclic stress.

TABLE I Details of specimens monotonically fractured after cycling for 1000 cycles without observable damage

Specimen	f_{cu}/f_{fc}	$(\sigma_{max}-f_{fc})/(f_{cu}-f_{fc})$
5-12	1.71	0.23
5-7	1.42	0.14
5-1	1.43	0.02
4-16	1.88	0.19

sight a chaotic behaviour that is summarized in the S–N plot shown in Fig. 9. Four speciments which did not fail after 1000 cycles and showed no significant degradation, with completely reversible crack opening behaviour, were subsequently fractured by monotonic loading. Their details are presented in Table I. It was found that all 4 of these specimens had comfortably large ranges between their first crack strengths f_{fc} and their maximum post-cracking strengths f_{cu} as shown in Table I, and that the actual cyclic excursions into the range f_{cu} to f_{fc} was in all cases equal to or less than 23%. Naturally, the corresponding fractional overloading of the fractured specimens into the range between the two cracking events could not be determined. It is, however, conjectured that, for those specimens, the penetration into this marginal range was in excess of 23% and was thus responsible for their progressive cyclic degradation and their eventual fracture.

The monitored cyclic crack opening displacements of specimens provided additional information. In Fig. 10a, a typical cyclic crack opening displacement is shown as a function of number of cycles for Specimen 5-1, which remained intact after 1000 cycles. No changes are apparent. Clearly, the cycling flexes the fibres in and out during every cycle without producing any further pull-out. In comparison, Fig. 10b shows a changing cyclic crack opening displacement of a specimen that has fatigued after about 525 cycles. The cyclic in and out flexing of the fibres is accompanied by a continued gradual pull-out of fibres until the specimen becomes unstable. This is followed by rapid tearing.

From these limited experiments it has become clear that in the absence of complicating environmental effects, continued cyclic degradation occurs only when the maximum stress per cycle penetrates sufficiently into the range between the first crack strength f_{fc} and post cracking maximum strength f_{cu}, i.e. when $(\sigma_{max}-f_{fc})>0.23\,(f_{cu}-f_{fc})$. The apparently chaotic behaviour in the tests reported above, then, is the result of

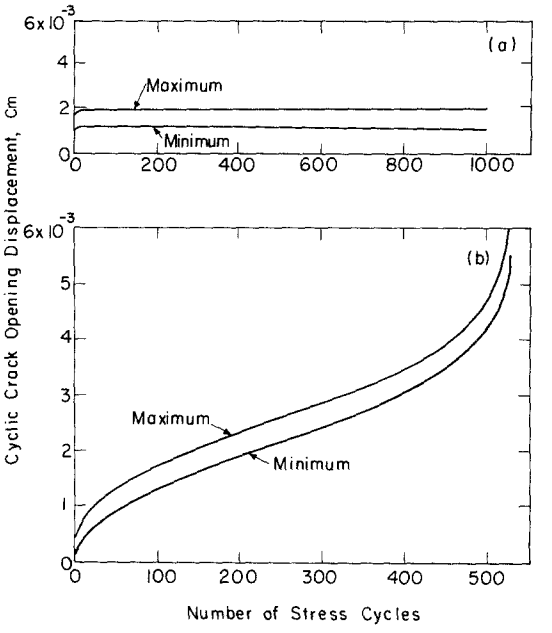

Figure 10(a) Stable crack opening displacement in specimen showing no increasing degradation and fatigue with further number of cycles; (b) continued cyclic fibre pull-out in specimen that has eventually fractured after 525 cycles.

the scatter in f_{cu} and f_{fc}, primarily due to variations in V_f between specimens and to a lesser degree due to variation in fibre orientation across the waist section of the specimens.

5. Discussion

The experiments presented above, utilizing Metglas in mortar, have broadly confirmed theoretical predictions of the behaviour of a cementitious material reinforced with discontinuous stiff metallic fibres. With Metglas fibres, the fundamental force–displacement relation of pull-out is readily measured. This relation shows that shear traction along the interface between roughened fibre and matrix, degrades considerably upon fibre pull-out. But once this basic information is known, the overall specimen separation behaviour by collective pull-out of fibres can be determined rather well by direct superposition, as was demonstrated in Fig. 8.

The experiments have demonstrated that the reinforcing fibres tend to raise the first crack strength rather gradually and according to the principle of non-propagating cracks, rather than the stress intensity concepts proposed by Romualdi and Batson [11], which would have had a different and stronger dependence on volume fraction of fibres.

The post cracking behaviour of the composites studied showed a leveling off behaviour at a volume fraction somewhat in excess of 0.01. This was due to a short circuiting of the fibre pull-out process by the development of small matrix cracks bridging between fibres in the pull-out process and thereby tearing out chunks of matrix stuck between such fibres. Thus, unless the fibre geometry could be altered or made wavy, or the matrix strength raised, it is of no advantage to incorporate larger volume fractions of fibre into the composite. In any event, for the given fibre aspect ratio and fibre shape it was not found possible to mix more than a volume fraction of 0.03 into the mortar in a uniform manner. Even for such modest volume fractions as 0.01, however, the specific fracture work could be increased more than 2000 fold over that of the unreinforced mortar.

The cyclic behaviour of the composite was also found to be remarkable. No progressive damage was found when the maximum stress excursion penetrated less than 23% into the range between the first crack strength and the maximum post crack strength. The cyclic experiments, however, were too few to reach sound conclusions about the fatigue process in such materials.

In the final analysis, a corrosion resistant high strength reinforcing material such as Metglas, that does not become embrittled upon scratching, demonstrates superior performance in reinforcement of cementitious materials.

Acknowledgements

This research was supported partly by Allied Chemical Corporation by means of fellowships for G.W.H. and H.Y.K., and by furnishing ample supplies of Metglas fibre. We are grateful to Dr J. J. Gilman for this support. The research was also supported in part by the National Science Foundation through the Center for Materials Science and Engineering, under Grant No. DMR 72-03027 A05.

References

1. H. KRENCHEL, "Fibre Reinforced Concrete", Publ. SP-44, (American Concrete Institute, Detroit, 1974), p. 45.
2. ACI Committee 544, *ACI J.* November (1973) 729.
3. National Physical Laboratory, "The Properties of Fibre Composites" (IPC Science and Technology Press, Guildford, Surrey, 1971), pp. 1–90.
4. American Concrete Institute, Fibre Reinforced Concrete, Publ. SP-44, (American Concrete Institute, Detroit, 1974) pp. 1–554.
5. A. NEVILLE (editor), "Fibre Reinforced Cement and Concrete" (RILEM Symposium 1975), (The Construction Press, Ltd., Hornby, Lancaster, 1975) pp. 1–459.
6. A. S. ARGON and W. J. SHACK, "Fibre Reinforced Cement and Concrete", edited by A. Neville (The Construction Press, Ltd., Hornby, Lancaster, 1975) p. 39.
7. J. P. ROMUALDI and J. A. MANDEL, *ACI J.* June (1964) 657.
8. A. J. MAJUMDAR, *Cement and Concrete Res.* 4 (1974) 247.
9. D. J. PINCHIN and D. TABOR, "Fibre Reinforced Cement and Concrete", edited by A. Neville, Vol. 2, (The Construction Press Ltd., Hornby, Lancaster, 1975), p. 521.
10. G. A. COOPER and J. M. SILLWOOD, *J. Mater. Sci.* 7 (1972) 325.
11. J. P. ROMUALDI and G. B. BATSON, *J. Eng. Mech. Div. Proc. ASCE* 89 (1963) 147.

Received 18 October and accepted 20 November 1978.